Tensorial Multi-view Subspace Clustering with Side Constraints for Elevator Security Warning

Huangzhen Xu
Huzhou special equipment inspection center
Licheng Ruan
Huzhou special equipment inspection center
Yuzhou Ni
Huzhou University
Hongwei Yin (02713@zjhu.edu.cn)
Huzhou University
Pu Yu
Huzhou special equipment inspection center
Xinmin Chen
Huzhou University

Research Article

Keywords: Multi-view clustering, Tensorial multi-view subspace learning, Adaptive graph learning, Side constraint, Elevator security warning

Posted Date: July 13th, 2023

DOI: https://doi.org/10.21203/rs.3.rs-3153565/v1

Additional Declarations: No competing interests reported.

Version of Record: A version of this preprint was published at Multimedia Systems on January 13th, 2024. See the published version at https://doi.org/10.1007/s00530-023-01234-3.

Tensorial Multi-view Subspace Clustering with Side Constraints for Elevator Security Warning

Huangzhen Xu[1], Licheng Ruan[1], Yuzhou Ni[2], Hongwei Yin[2*], Ping Yu[1], Xinmin Cheng[2]

[1]Huzhou special equipment inspection center, Huzhou, 313000, China.
[2]College of Information Engineering, Huzhou University, Huzhou, 313000, China.

*Corresponding author(s). E-mail(s): 02713@zjhu.edu.cn;

Abstract

In recent years, using clustering technology to realize equipment security warning is a research hotspot in the field of data mining applications. However, due to the lack of data fusion mechanism and prior knowledge guidance, the performance of most existing methods is limited when applied to complex equipment such as elevator. In this paper, a novel **T**ensorial **M**ulti-view **S**ubspace **C**lustering with **S**ide constraints (TMSCS) is proposed for elevator security warning, which first introduces tensorial multi-view subspace learning to achieve data fusion based on high-order correlation. Secondly, the prior knowledge is formalized as side constraints between samples through adaptive graph learning, where certain elevators is forced to have similar or dissimilar operation status. Thirdly, a unified model combining tensorial multi-view subspace learning and adaptive graph learning is constructed to eliminate the instability caused by phased learning. Furthermore, an efficient optimization algorithm is designed to solve this model. Extensive experiments on several benchmark datasets demonstrate the superiority of our method, and the experimental results on real elevator status datasets demonstrate that our method accurately identifies the operating status of each elevator equipment.

Keywords: Multi-view clustering, Tensorial multi-view subspace learning, Adaptive graph learning, Side constraint, Elevator security warning

1 Introduction

Different from general industrial equipment, elevator is used more widely and frequently in people's daily life, where its related accidents cause unbearable loss of property and life. Elevator security warning is an important topic in the special equipment supervision [1]. With the rapid growth of elevator ownership, traditional security warning methods that rely on manual detection, key indicators and statistical analysis no longer meet the practical needs. It's necessary to improve the efficiency and accuracy of elevator security warning through data mining technology [2–4]. On the other hand, market or government regulators effectively monitor the operating status of elevators through multiple data sources. By collecting these elevator status data resources, these government regulators aim to comprehensively and accurately identify the operating status of a large number of elevator equipments at the same time. Because of the natural semantic gap between different data sources and the difficulty of label acquisition, unsupervised data fusion and learning

method is the key technology for utilizing these data resources.

As a typical unsupervised data fusion and learning method, multi-view clustering (MVC) achieves semantic-level data fusion by leveraging the consistency and complementarity among multiple views, while obtaining the comprehensive latent data distribution [5–11]. Many advanced MVC methods have been proposed and some practical cases demonstrate their effectiveness [12–15]. For the elevator security warning task, the status data collected from different sources is regarded as the feature description of different views, called multi-view elevator status data. In [16], we construct a elevator security warning framework based on multi-view nonnegative matrix factorization, where the security status of a elevator equipment is determined by analyzing the cluster in which it is located. However, the performance of the proposed method in [16] still cannot meet the practical elevator security warning. Two major reasons that limit its performance include: 1) Multi-view elevator status data suffers from low signal-to-noise ratio due to sensor failures, transmission interference, and human tampering. These noises and outliers severely degrade the performance of multi-view clustering. 2) Due to the sparse features of elevator status data, it is difficult to obtain its latent distribution only by unsupervised clustering models. Considering the important guiding role of prior knowledge in judging the elevator operation status, it is necessary to incorporate the prior knowledge. Existing tensorial multi-view clustering approaches cannot directly handle prior knowledge properly [17–19].

To solve these problems, a novel **T**ensorial **M**ulti-view **S**ubspace **C**lustering with **S**ide constraints (TMSCS) is proposed in this paper. First, tensorial multi-view subspace learning is utilized to obtain the self-expressive subspace representation of each view, where the tensor low-rank constraint enhances the ability to deal with noise by capturing high-order correlations. Second, through adaptive graph learning, prior knowledge is incorporated into our model as side constraints, including must-link and cannot-link constraints. Then, a unified model combining tensorial multi-view subspace learning and adaptive graph learning is constructed to eliminate the instability caused by phased learning. Finally, classical spectral clustering is conducted on the similarity matrix obtained from our model, and the security level of each elevator is determined according to the clustering results. The framework is shown in Fig. 1, and the main contributions of this paper are summarized as follows:

- This paper proposes a unified multi-view clustering model that combines tensorial multi-view subspace learning and adaptive graph learning. The prior knowledge is formalized as a hybrid matrix in adaptive graph learning, containing both must-link and cannot-link side constraints. By forcing similarity matrix to be consistent with this hybrid matrix, prior knowledge is effectively integrated into our model while preserving the raw data intrinsic structure.
- For low signal-to-noise ratio, the tensor low-rank constraint is introduced to capture the high-order correlations among multiple views. In addition to the use of l_{21} norm, the subspace representation learning of different views is not carried out independently, but combined into a single tensor whose global low-rank property is achieved by tensor tucker decomposition.
- An effective algorithm based on alternating optimization strategy is proposed to solve the unified model. Moreover, extensive experiments on benchmark datasets show the effectiveness of our method, where the proposed method successfully achieves data fusion and accurately captures the latent distribution. Experiments on real multi-view elevator state status datasets validate that our method can identify the elevator security level.

The rest is organized as follows: Section 2 briefly introduces the related work including tensorial multi-view clustering and Semi-supervised multi-view clustering, Section 3 describes our proposed method in detail, Section 4 records and analyzes the experimental results, and Section 5 summarizes this paper.

2 Related Works

In the past decade, some representative research works are proposed to improve the performance of multi-view clustering, in which learning a tensor with compact low-rank structure will well exploit the complementary information and high-order correlation among multi-view data. In [7], it first treats each self-expressive subspace as a

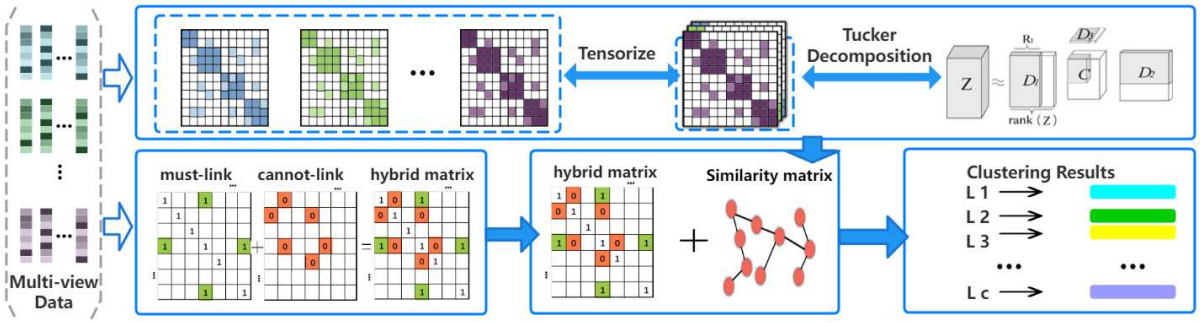

Fig. 1 Main framework: First, the subspace representation $\mathcal{Z}$ is obtained by tensorial multi-view subsapce learning, where its global low-rank property is achieved by Tucker decomposition. Secondly, the target similarity matrix is obtained by adaptive graph learning, where the prior knowledge includings must-link and cannot-link constraints is formalized as a hybrid matrix. Finally, the spectral clustering is conducted on the target similarity matrix to obtain clustering results.

slice of a third-order tensor, and then imposes tensor low-rank constraint on it. [8] proposes a novel tensor multi-rank minimization framework to ensure the consistency of multi-view data. In [9], a unified multi-view clustering model that simultaneously learns low-rank tensor representations and affinity matrices is proposed. Furthermore, [20] proposes a one-step multi-view clustering model via skinny tensor learning and latent clustering, which enforces the synergistic interaction between tensor representation learning and clustering processes. [10] combines Markov chains with tensor to enhance the robustness of low-rank tensor. In [18], a better surrogate of tensor rank is designed, namely the tensor logarithmic Schatten-p norm, which fully considers the physical difference between singular values by the non-convex and non-linear penalty function.

Semi-supervised multi-view clustering is also an important research direction in the field of cluster analysis. Through the guidance of prior knowledge, the performance of semi-supervised multi-view clustering model can be significantly improved. When incorporating prior knowledge into a specific learning model, it is necessary to design a guidance mechanism according to the characteristics of the specific model. In [11], adaptive graph learning is introduced to semi-supervised MVC, which obtains the neighborhood relationship of each sample. Similarly, [21] aims to find latent multi-view representation by graph learning and label propagation. In [22], an exclusive nonnegative subspace learning model is proposed, which is extended to semi-supervised MVC by using manifold regularization. In [16] combines constrained nonnegative matrix factorization with low-rank representation to enhance clustering performance. [23] employs label propagation mechanism based on the stream structure to make full use of the limited label information. In semi-supervised multi-view clustering, the key is to establish the relationship between prior knowledge and clustering model, that effectively extracts knowledge from the prior information to promote the separation between clusters.

According to the characteristics of multi-view elevator status data, tensorial multi-view subspace learning is extended to semi-supervised clustering scenario in this paper. Specially, tensorial multi-view subspace learning with low rank constraint can deal with noise well, while the semi-supervised mechanism based on adaptive graph learning can greatly improve the accuracy of clustering. Based on the above two reasons, the main motivation of this paper is to build a unified model to form a collaborative interaction between these two approaches, and then improve the elevator security warning ability.

3 Methodology

3.1 Tensorial multi-view subsapce learning

Multi-view subspace clustering focuses on learning a latent shared subspace representation as the common similarity matrix of multi-view data, and then performing spectral clustering on the similarity matrix to obtain clustering results. Given a multi-view dataset $\{\mathbf{X}^v\}_{v=1}^m$, where $\mathbf{X}^v \in \mathcal{R}^{d^v \times n}$

is the feature matrix of v-th view, d^v is the feature dimension of v-th view, n is the number of samples and m is the number of views. Let $\mathbf{Z}^v$ and $\mathbf{E}^v$ respectively denote the self-expressive subspace representation and noises of v-th view. With the self-expressive property, the general model of multi-view subspace clustering is formulated as:

$$\begin{aligned} &\min_{\mathbf{Z}^v,\mathbf{E}^v} \sum\nolimits_{v=1}^{m} \|\mathbf{E}^v\| + \Omega(\mathbf{Z}^1,\ldots,\mathbf{Z}^m) \\ &s.t.\ \ \mathbf{X}^v = \mathbf{X}^v\mathbf{Z}^v + \mathbf{E}^v,\ \forall v \end{aligned} \tag{1}$$

where $\Omega(\mathbf{Z}^1,\ldots,\mathbf{Z}^m)$ is the regularizer for multi-view subspace representation with respect to different structural properties, such as l_1 norm [24] or nuclear norm [25]. $\|\mathbf{E}^v\|$ is the error metric of noises and outliers. This matrix-oriented general model is unable to explore high-order correlation across multiple views.

Based on tensor construction technique, all view-specific subspace representations are composed into a third-order tensor, where the final performances are jointly optimized in a mutual manner [7, 26]. With the tensor low-rank constraint, the general model of multi-view subspace clustering are formulated as follows:

$$\begin{aligned} &\min_{\mathcal{Z},\mathbf{E}^v} \|\mathcal{Z}\|_{\circledast} + \sum\nolimits_{v=1}^{m} \|\mathbf{E}^v\| \\ &s.t.\ \ \mathbf{X}^v = \mathbf{X}^v\mathbf{Z}^v + \mathbf{E}^v,\ \forall v \\ &\qquad\ \ \mathcal{Z} = \psi(\mathbf{Z}^1,\mathbf{Z}^2,\cdots,\mathbf{Z}^m) \end{aligned} \tag{2}$$

where $\psi(\cdot)$ merges view-specific subsapce representations $\mathbf{Z}^v$ into a $n\times n\times m$ tensor $\mathcal{Z}$. $\|\mathcal{Z}\|_{\circledast}$ is the tensor nuclear norm of $\mathcal{Z}$, which is a convex combination of the nuclear norms of all matrices unfolded along each mode. $\|\mathcal{Z}\|_{\circledast}$ imposes the low-rank constraint to the subspace representation.

3.2 Adaptive graph learning

For a certain $\mathbf{X}^v$ in the above multi-view dataset, its local structure information can be obtained by adaptive graph learning [27–29]. Considering each sample as a node on the graph, the connection probability of two nodes is the similarity between them. When $\mathbf{x}_i^v$ and $\mathbf{x}_j^v$ are connected with probability w_{ij}^v, then w_{ij}^v represents their similarity. Let $\mathbf{W}^v$ denote the connection probability matrix on graph, and $\mathbf{L}^v = \mathbf{D}^v - (\mathbf{W}^v + (\mathbf{W}^v)^T)/2$ denote its corresponding Laplace matrix. Noted that $\mathbf{D}^v = diag\left(d_1^v, d_2^v, ..., d_n^v\right)$ is the degree matrix, where $d_i^v = \sum_{j=1}^{n} w_{ij}^v$ is the degree of i-th node. With local structure preservation, the adaptive graph learning is generally as:

$$\begin{aligned} &\min_{\mathbf{W}^v} Tr((\mathbf{X}^v)^T\mathbf{L}^v\mathbf{X}^v) + \|\mathbf{W}^v\|_F^2 \\ &s.t.\ (\mathbf{W}^v)^T\mathbf{1} = \mathbf{1},\ \mathbf{0} \le \mathbf{W}^v \le \mathbf{1} \end{aligned} \tag{3}$$

Through simple mathematical transformation, the above formula can be converted into:

$$\begin{aligned} &\min_{\mathbf{W}^v} \sum\nolimits_{i,j=1}^{n} \frac{1}{2}\left\|\mathbf{x}_i^v - \mathbf{x}_j^v\right\|_2^2 w_{ij}^v + (w_{ij}^v)^2 \\ &s.t.\ \mathbf{1}^T\mathbf{w}_i^v = 1,\ 0 \le \mathbf{w}_i^v \le 1,\ \forall i \end{aligned} \tag{4}$$

For convenience, with $p_{ij}^v = \frac{1}{2}||x_i^v - x_j^v||_2^2$, then we have the following formulation:

$$\begin{aligned} &\min_{\mathbf{W}^v} \sum\nolimits_{i,j=1}^{n} p_{ij}^v w_{ij}^v + \sum\nolimits_{i,j=1}^{n} (w_{ij}^v)^2 \\ &s.t.\ \mathbf{1}^T\mathbf{w}_i^v = 1,\ 0 \le \mathbf{w}_i^v \le 1,\ \forall i \end{aligned} \tag{5}$$

Denote $\mathbf{p}_i^v \in \mathcal{R}^{n\times 1}$ as a vector with j-th element as p_{ij}^v. Since each column $\mathbf{w}_i^v$ in matrix $\mathbf{W}^v$ is independent, Eq.(5) is equivalent to the following quadratic programming problem, which can be solved with a closed form solution as in [29].

$$\begin{aligned} &\min_{\mathbf{w}_i^v} \left\|\mathbf{w}_i^v + \frac{\mathbf{p}_i^v}{4}\right\|_2^2 \\ &s.t.\ \mathbf{1}^T\mathbf{w}_i^v = 1,\ 0 \le \mathbf{w}_i^v \le 1,\ \forall i \end{aligned} \tag{6}$$

3.3 Formulation

In elevator security warning, prior knowledge is usually generated in the form of side constraint between samples, which consists of must-link and cannot-link constraints. Must-link constraint means that two elevators should have the same operating status and belong to the same cluster, while the cannot-link constraint means that two elevators should have different operating status and belong to different clusters. Then, an hybrid matrix $\tilde{\mathbf{W}}$ with two side constraints is defined as:

$$\tilde{w}_{ij}^v = \begin{cases} 1 & \text{if } (\mathbf{x}_i, \mathbf{x}_j) \text{ must link} \\ 0 & \text{if } (\mathbf{x}_i, \mathbf{x}_j) \text{ cannot link} \\ w_{ij}^v & \text{otherwise} \end{cases} \tag{7}$$

To improve the structural representation ability of the obtained similarity matrix and eliminate the instability caused by phased learning, a unified model combining tensorial multi-view subspace learning and adaptive graph learning is constructed. The target similarity matrix is forced to agree with the above hybrid matrix to incorporate side constraints. The objective function is expressed as follows:

$$\begin{aligned}\min_{\mathcal{Z},\mathbf{E},\mathbf{S}} &\|\mathcal{Z}\|_{\circledast}+\alpha\|\mathbf{E}\|_{2,1}+\beta\left\|\mathbf{S}-\tilde{\mathbf{W}}\right\|_F^2 \\ &+\gamma\sum_{v=1}^{m}Tr\left((\mathbf{Z}^v)^T\mathbf{L_S}\mathbf{Z}^v\right) \\ s.t.&\begin{cases}\mathbf{X}^v=\mathbf{X}^v\mathbf{Z}^v+\mathbf{E}^v \\ \mathcal{Z}=\psi\left(\mathbf{Z}^1,\mathbf{Z}^2,\ldots,\mathbf{Z}^m\right) \\ \mathbf{E}=\left[\mathbf{E}^1;\mathbf{E}^2;\ldots;\mathbf{E}^m\right] \\ \mathbf{S}^{\mathrm{T}}\mathbf{1}=\mathbf{1},\mathbf{0}\le\mathbf{S}\le\mathbf{1}\end{cases}\end{aligned} \tag{8}$$

where the first two terms are the tensorial multi-view subspace learning. $\mathbf{E}=\left[\mathbf{E}^1;\mathbf{E}^2;\ldots;\mathbf{E}^m\right]$ is formed by concatenating together along the column of error metric matrices. To alleviate the influence of noises, a structured sparsity l_{21} norm regularization is imposed on $\mathbf{E}$, which encourages its columns to be zero. Afterwards, the low rank property of tensor $\mathcal{Z}$ is achieved by using Tucker decomposition. The second term is the adaptive graph learning. Obviously, through this mechanism, the local structure information of multi-view data can be efficiently fused. In third term, the side constraints are incorporated into our model by minimizing the difference between target similarity matrix $\mathbf{S}$ and auxiliary hybird matrix $\tilde{\mathbf{W}}$.

3.4 Optimization

Since the above non-convex objective function is difficult to optimize directly, the Augmented Lagrange Method with alternating direction minimizing strategy (AL-ADM) is adopted to solve this problem. The other variables are always fixed in each iteration while only one variable is updated. To make the objective function separable, an auxiliary tensor $\mathcal{G}=\psi\left(\mathbf{G}^1,\mathbf{G}^2,\ldots,\mathbf{G}^m\right)$ is introduced to replace $\mathcal{Z}$, and the objective function in Eq.(8) is transformed into:

$$\begin{aligned}\min_{\mathcal{Z},\mathbf{E},\mathbf{S},\mathcal{G}} &\|\mathcal{Z}\|_{\circledast}+\alpha\|\mathbf{E}\|_{2,1}+\beta\left\|\mathbf{S}-\tilde{\mathbf{W}}\right\|_F^2 \\ &+\gamma\sum_{v=1}^{m}Tr\left((\mathbf{G}^v)^T\mathbf{L_S}\mathbf{G}^v\right) \\ s.t.&\begin{cases}\mathbf{X}^v=\mathbf{X}^v\mathbf{G}^v+\mathbf{E}^v \\ \mathcal{Z}=\psi\left(\mathbf{Z}^1,\mathbf{Z}^2,\ldots,\mathbf{Z}^m\right) \\ \mathcal{G}=\psi\left(\mathbf{G}^1,\mathbf{G}^2,\ldots,\mathbf{G}^m\right),\ \mathcal{G}=\mathcal{Z} \\ \mathbf{E}=\left[\mathbf{E}^1;\mathbf{E}^2;\ldots;\mathbf{E}^m\right] \\ \mathbf{S}^T\mathbf{1}=\mathbf{1},\ \mathbf{0}\le\mathbf{S}\le\mathbf{1}\end{cases}\end{aligned} \tag{9}$$

The corresponding unconstrained optimization problem of the above function is to minimize the following augmented Lagrangian function:

$$\begin{aligned}&\mathcal{L}_\rho\left(\mathcal{Z};\mathbf{S};\{\mathbf{E}^v\}_{v=1}^m;\{\mathbf{G}^v\}_{v=1}^m\right)= \\ &\|\mathcal{Z}\|_{\circledast}+\alpha\sum_{v=1}^{m}||\mathbf{E}^{\mathrm{v}}||_{2,1}+\beta\left\|\mathbf{S}-\tilde{\mathbf{W}}\right\|_F^2 \\ &+\gamma\sum_{v=1}^{m}Tr((\mathbf{G}^v)^T\mathbf{L_S}\mathbf{G}^v)+\Phi(\mathcal{W},\mathcal{Z}-\mathcal{G}) \\ &+\sum_{v=1}^{m}\Phi((\mathbf{U}^v)^T,\mathbf{X}^v-\mathbf{X}^v\mathbf{G}^v-\mathbf{E}^v)\end{aligned} \tag{10}$$

where $\mathcal{W}$ and $\mathbf{U}^v$ are lagrange multipliers. For ease, $\Phi(\mathcal{W},\mathcal{Z}-\mathcal{G})=\frac{\rho}{2}||\mathcal{Z}-\mathcal{G}||_F^2+<\mathcal{W},\mathcal{Z}-\mathcal{G}>$ and $\Phi((\mathbf{U}^v)^T,\mathbf{X}^v-\mathbf{X}^v\mathbf{G}^v-\mathbf{E}^v)=\frac{\rho}{2}||\mathbf{X}^v-\mathbf{X}^v\mathbf{G}^v-\mathbf{E}^v||_F^2+<(\mathbf{U}^v)^T,\mathbf{X}^v-\mathbf{X}^v\mathbf{G}^v-\mathbf{E}^v>$, where $<\cdot,\cdot>$ is the matrix inner product and ρ is a penalty parameter. Next, the specific optimization steps are derived.

For updating $\mathbf{G}^v$. When other variables are fixed, the Eq.(10) is equivalent to the following optimization problem:

$$\begin{aligned}\mathbf{G^{v*}}=\min_{\mathbf{G^v}}&\gamma\sum_{v=1}^{m}Tr((\mathbf{G}^v)^T\mathbf{L_S}\mathbf{G}^v) \\ &+\frac{\rho}{2}||\mathcal{Z}-\mathcal{G}+\frac{\mathcal{W}}{\rho}||_F^2 \\ &+\frac{\rho}{2}\sum_{v=1}^{m}||\mathbf{X}^v-\mathbf{X}^v\mathbf{G}^v-\mathbf{E}^v+\frac{\mathbf{U}^v}{\rho}||_F^2\end{aligned} \tag{11}$$

Setting the derivative with respect to $\mathbf{G^v}$ to 0, its closed-form solution is:

$$\begin{aligned}\mathbf{G}^{v*}=&(\rho(\mathbf{I}+(\mathbf{X}^v)^T\mathbf{X}^v)+2\gamma\mathbf{L_s})^{-1} \\ &(\rho\mathbf{Z}^v+\mathcal{W}+\rho(\mathbf{X}^v)^T(\mathbf{X}^v-\mathbf{E}^v+\frac{\mathbf{U}^v}{\rho}))\end{aligned} \tag{12}$$

For updating $\mathbf{E}^v$: When other variables are fixed, as in [9], $\mathcal{L}$ is solved by:

$$\begin{aligned}\mathbf{E}^* =& \min_{\mathbf{E}} \sum_{v=1}^{m} \alpha||\mathbf{E}^{\mathrm{v}}||_{2,1} \\ &+ \sum_{v=1}^{m} \Phi((\mathbf{U}^v)^T, \mathbf{X}^v - \mathbf{X}^v\mathbf{G}^v - \mathbf{E}^v) \\ =& \min_{\mathbf{E}} \frac{\alpha}{\rho}||\mathbf{E}||_{2,1} + \frac{1}{2}||\mathbf{E} - \mathbf{F}||_F^2\end{aligned} \tag{13}$$

where $\mathbf{E}$ is $[\mathbf{E}^1; \mathbf{E}^2; ...; \mathbf{E}^v]$. $\mathbf{F}$ is formed by concatenating the matrix $\mathbf{F}^v = \mathbf{X}^v - \mathbf{X}^v\mathbf{G}^{\mathrm{v}} + \mathbf{U}^v/\rho$ vertically along the columns. Using Lemma 3.2 in [30] can effectively solve this subproblem. In t-th iteration, the j-th column of $\mathbf{E}$ is obtained by:

$$\mathbf{E}_{t+1}(:,j) = \begin{cases} \frac{\|\mathbf{F}_t(:,j)\|_2 - \frac{1}{\rho_t}}{\|\mathbf{F}_t(:,j)\|_2}\mathbf{F}_t(:,j), & \text{if } \frac{1}{\rho_t} < \|\mathbf{F}_t(:,j)\|_2 \\ 0, & \text{otherwise} \end{cases} \tag{14}$$

For updating $\mathcal{Z}$: When other variables are fixed, $\mathcal{L}$ is solved by:

$$\begin{aligned}\mathcal{Z}^* &= \min_{\mathcal{Z}^*} \|\mathcal{Z}\|_{\circledast} + \Phi(\mathcal{W}, \mathcal{Z} - \mathcal{G}) \\ &= ||\mathcal{Z} - (\mathcal{G} - \frac{\mathcal{W}}{\rho})||_F^2 \\ s.t.&\ \ \mathcal{Z} = \mathcal{C} \times_1 \mathbf{D}_1 \times_2 \mathbf{D}_2 \times_3 \mathbf{D}_3,\ \mathbf{D}_i' * \mathbf{D}_i = \mathbf{I}.\end{aligned} \tag{15}$$

here we use the classical Tucker decomposition to solve this optimization problem. In Tucker decomposition, a tensor is represented by a core tensor multiplied by a matrix along each mode. A third-order tensor $\mathcal{Z} \in \mathbb{R}^{I \times J \times K}$ can be decomposed into three factor matrices $\mathbf{D}_1 \in \mathbb{R}^{I \times P}, \mathbf{D}_2 \in \mathbb{R}^{J \times Q}, \mathbf{D}_3 \in \mathbb{R}^{K \times R}$ and a core tensor $\mathcal{C} \in \mathbb{R}^{P \times Q \times R}$. The details are shown in Definition 3 of [9]. As in [31], the core tensor $\mathcal{C}'$ and the orthogonal factor matrix $\mathbf{D}_i'$, $i = 1, 2, 3$ of $\mathcal{G} - \frac{\mathcal{W}}{\rho}$ are obtained by Higher-Order Orthogonal Iteration algorithm (HOOI). Thus, the low-rank representation $\mathcal{Z}^*$ is obtained as:

$$\mathcal{Z}^* = \mathcal{C}' \times {}_1\mathbf{D}_1' \times {}_2\mathbf{D}_2' \times {}_3\mathbf{D}_3' \tag{16}$$

For updating $\mathbf{S}$: When other variables are fixed, $\mathcal{L}$ is solved by:

$$\mathbf{S}^* = \min_{\mathbf{S}^*} \gamma \sum_{v=1}^{m} Tr((\mathbf{G}^v)^T\mathbf{L}_{\mathbf{S}}\mathbf{G}^v) + \beta \left\|\mathbf{S} - \tilde{\mathbf{W}}\right\|_F^2 \tag{17}$$

Algorithm 1 Tensorial Multi-view Subspace Clustering with Side Constraints for Elevator Security Warning (TMSCS)

Input Data matrix $X^1, X^2, ..., X^v$, the number of nearest neighbors k, trade-off parameter α, β and γ, side information matrix $\tilde{W}$.
Initialize $\mathbf{G}^v = \mathbf{E}^v = \mathbf{U}^v = \mathbf{S} = \mathcal{Z} = \mathcal{W} = \mathbf{0}$; $\rho = 10^{-1}$; $\mu = 1.5$; $\varepsilon = 10^{-3}$; $\rho_{\max} = 10^{10}$
Using Eq.(6) and Eq.(7) to obatin auxiliary hybird matrix $\tilde{\mathbf{W}}$
while not converge **do**
  for each view v **do**
    Update $\mathbf{G}^{\mathbf{v}}$ by using Eq.(12);
    Update $\mathbf{E}^{\mathbf{v}}$ by using Eq.(13);
    Update $\mathbf{S}$ by using Eq.(20);
  end for
  Update $\mathcal{Z}$ by using Eq.(16);
  Update $\mathbf{U}^v$ and $\mathcal{W}$ by using Eq.(21);
  Check the convergence conditions:
  $\max \left\{ \begin{array}{l} ||X^v - X^vG^v - E^v||_\infty \\ ||\mathcal{Z} - \mathcal{G}||_\infty \end{array} \right\} \leq \varepsilon$

end while
Output Affinity matrix by $(\mathbf{S} + \mathbf{S}^{\mathbf{T}})/\mathbf{2}$.

where the first term in the above formula can be expanded as $\frac{\gamma}{2}\sum_{v=1}^{m}(\sum_{i,j=1}^{n}\left\|\mathbf{g}_i^v - \mathbf{g}_j^v\right\|_F^2 \mathbf{s}_{ij})$. For simplicity, let $b_{ij}^v = ||\mathbf{g}_i^v - \mathbf{g}_j^v||_2^2$, which forms a matrix $\mathbf{B}^v$. Let $\mathbf{A} = 2\tilde{\mathbf{W}} - \frac{\gamma}{2\beta}\mathbf{B}$, then the Eq.(17) is equivalent to:

$$\min_{\mathbf{S}^T\mathbf{1}=\mathbf{1}, 0 \leq \mathbf{S} \leq 1} Tr(\mathbf{S}^T\mathbf{S}) - Tr(\mathbf{S}^T\mathbf{A}) \tag{18}$$

The vector form of Eq.(18) is rewritten as:

$$\min_{\mathbf{s}_i^T\mathbf{1}=1, 0 \leq \mathbf{s}_i \leq 1} \sum_{i=1}^{n} (\mathbf{s}_i^T\mathbf{s}_i - \mathbf{s}_i^T\mathbf{a}_i) \tag{19}$$

where s_i and a_i represent the i-th rows of matrices $\mathbf{S}$ and $\mathbf{A}$, respectively. Since each s_i is independent, Eq.(19) is decomposed into n subproblems as follows:

$$\min_{\mathbf{s}_i^T\mathbf{1}=1, 0 \leq \mathbf{s}_i \leq 1} (\mathbf{s}_i^T\mathbf{s}_i - \mathbf{s}_i^T\mathbf{a}_i) \tag{20}$$

Noted that this optimization can be solved by Euclidean projection on the simplex method with closed-form solution in [32].

For Updating $\mathbf{U}^{v*}, \mathcal{W}^*, \rho^*$:

$$\begin{aligned} \mathbf{U}^{v*} &= \mathbf{U}^v + \rho(\mathbf{X}^v - \mathbf{X}^v\mathbf{G}^v - \mathbf{E}^v); \\ \mathcal{W}^* &= \mathcal{W} + \rho(\mathcal{Z} - \mathcal{G}); \\ \rho^* &= \min(\rho\mu, \rho_{\max}) \end{aligned} \tag{21}$$

where $\mu > 1$ is a penalty parameter, and $\rho_{\max}$ is the maximum value of ρ. The entire algorithm is summarized in Algorithm 1.

3.5 Complexity Analysis

There are four subproblems in the optimization process of our model. Firstly, updating the $\mathbf{G}^v$ requires matrix inversion and the Sylvester equation, both of which have complexity $\mathcal{O}\left(mn^3\right)$ and m is the number of views. Secondly, updating $\mathbf{E}^v$ and $\mathbf{U}^v$ involves matrix multiplication with complexity $\mathcal{O}(mn^2)$. Thirdly, updating $\mathcal{Z}$ involves the Tucker decomposition with complexity $\mathcal{O}(rmn^2)$, where r is the rank of Z^v. Fourthly, updating $\mathbf{S}$ has complexity $\mathcal{O}(mn^2)$. Therefore, the total complexity is $\mathcal{O}\left(mn^2\left(\mathrm{n}+r\right)\right)$. In addition, empirical evidence from real data shows that our algorithm has stable convergence behavior.

4 Experiment

4.1 Datasets

Here, we introduce three public datasets and three elevator datasets along with the multi-view features used for each. Sample images from three public datasets are shown in Fig.2.

Three public datasets are used: ORL[1], BBCsport[2], MSRC_v1[3]. Three elevator datasets: Elevator_CX, Elevator_WX, and Elevator_2022. The details of all datasets are shown in Table 1. The details of datasets are described below.

MSRC_v1 is an object database which contains 210 images from 7 categories including car, bicycle, airplane, building, face, tree and cow. This experiment sets 5 types of feature, including 24-D CM, 576-D HOG, 512-D GIST, 256-D LBP and 254-D CENT are extracted from each image.

ORL is a face database which contains 300 images of 40 distinct people. These images are taken at different times with varied lighting, facial expressions, and facial details. This experiment sets 3 types of feature(4096 Intensity, 3304 LBP , and 6750 Gabor).

BBCsport contains 544 sports new articles collected from 5 topical areas, which correspond to 5 classes including athletics, cricket, football, rugby and tennis. The document is described by two views, and dimensions of each view are 3283 and 3183 respectively.

Elevator_WX is a multi-view dataset contains 385 samples from Huzhou special equipment inspection center, which collected from Wuxing District, Huzhou City, Zhejiang Province, China. Each sample contains three views: a production view based on manufacturing data, an environmental view based on the special equipment installation environment and a maintenance view based on regular manual inspections. Furthermore,each sample has a risk level, which is divided into high-risk, medium-risk and low-risk equipments.

Elevator_CX is a multi-view dataset contains 427 samples from Huzhou special equipment inspection center, which collected from Changxing District, Huzhou City, Zhejiang Province, China. Each sample in these datasets consists of three views: production, environmental and maintenance. In addition, each sample has a risk level, which is divided into high-risk, medium-risk and low-risk equipments.

Elevator_2022 contains 709 samples is from the elevator data collected based on the Internet of Things equipment provided by Huzhou special equipment inspection center in April 2022, which collected from Wuxing District, Huzhou City, Zhejiang Province, China. Each sample contains 17 operating fault information, and each fault information is a feature. We collected 30 days' running information and took each day's running information as a view. According to the frequency of elevator failures in practical application scenarios and combined with expert experience, we divide elevators into three different levels: high-risk, medium-risk and low-risk. Table 2 lists the weight of fault features.

4.2 Compared methods

The method in this paper (TMSCS) compared with other algorithms, including two multi-view

[1] http://www.uk.research.att.com/facedatabase.html
[2] http://www.uk.research.att.com/facedatabase.html
[3] https://www.cnblogs.com/picassooo/p/12890078.html

Fig. 2 Sample images of three used datasets

Table 1 Multi-view datasets.

Dataset	Size	View	Cluster	View1	View2	View3	View4	View5
MSRC_v1	210	5	7	ms(24)	ms2(576)	ms3(512)	ms4(256)	ms5(254)
ORL	300	3	40	or1(4096)	or2(3304)	or3(6750)	/	/
BBCSport	544	2	5	bc1(3183)	bc2(3203)	/	/	/
Elevator_WX	385	3	3	el1(12)	el2(16)	el03(307)	/	/
Elevator_CX	427	3	3	el1(12)	el2(16)	el03(307)	/	/
Elevator_2022	709	30	3	/	/	/	/	/

nearest neighbor algorithms, one unsupervised tensor algorithm, and three semi-supervised algorithms. The multi-view nearest neighbor algorithms include: Graph Learning for Multiview Clustering(MVGL)[6], Multi-View Clustering and Semi-Supervised Classification with Adaptive Neighbours (MLAN)[11]. The unsupervised tensor algorithm includes: Low-Rank Tensor Graph Learning for Multi-view Subspace Clustering(LRTG)[9]. The semi-supervised algorithms include: tensorial Multi-view Subspace Representation Learning(TMSRL)[28], Constrained nonnegative matrix factorization for image representation(CNMF)[33], Constrained Low-Rank Representation for Robust Subspace Clustering(CLRR)[34].

4.3 Results on public datasets

This paper uses three common clustering metrics to measure the performance of the algorithms: normalized mutual information (NMI), accuracy (ACC), and adjusted rank index (AR), with higher values indicating better clustering performance. In this experiment, each algorithm was run ten times on the datasets and presented in the "mean ± standard deviation" format. In addition, "-" indicates that the algorithm cannot be applied to the dataset. The results are shown in Table 3:

- Compared with unsupervised tensor algorithm LRTG, our method combines semi-supervised information to get better results. The improvement rates of each dataset measured by ACC are 6%, 18%, 9%, 0.05% and 4%, respectively.
- Compared with other semi-supervised algorithms (CLRR, CNMF, TMSRL), TMSCS is better than CLRR in each dataset. It could improve by 12%, 7%, 3%, 0.03% and 2% in ACC. This phenomenon suggests that TMSCS explore correlations among multiple views more effectively. Besides, we observe that the clustering performance of the proposed method is better than most compared multi-view clustering methods. At its core, our method stacks

Table 2 Weight table of fault features.

Fault name	Fault weight
Topping	1
Battery car alarm	1
Jump fight alarm	1
Gate area outside elevator	1
Squat Bottom	1
Safety loop in upper limit zone is disconnected	9999
Hall door cannot open trapped person	9999
Safety loop break when the elevator is running	1
Safety loop disconnected	333
Open the door in operation	1
Door opening failure	1
Open the door and take the ladder	1
Other faults that prevent the elevator from restarting	1
Door lock disconnects	333
Door closing fault	1
Trapped	333

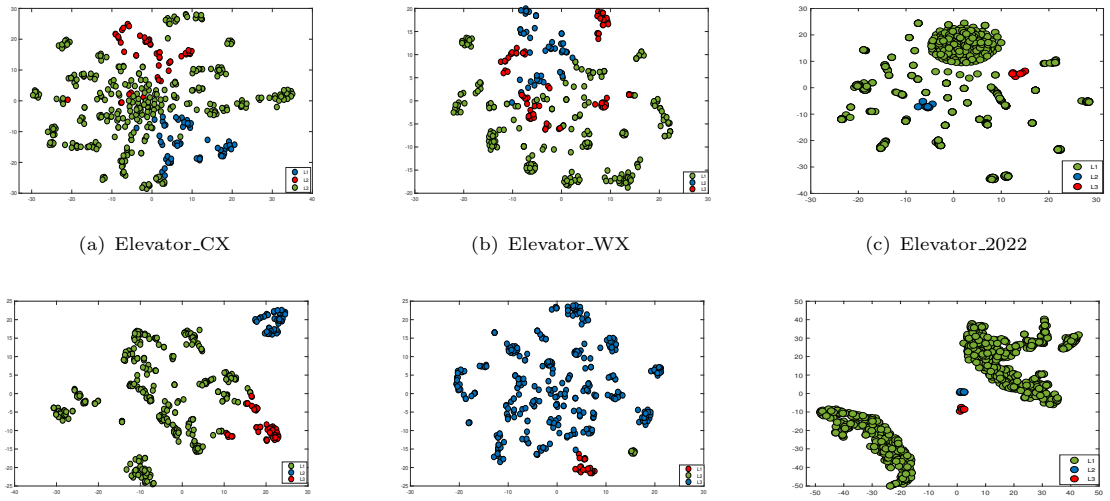

(a) Elevator_CX (b) Elevator_WX (c) Elevator_2022

(d) Elevator_CX (e) Elevator_WX (f) Elevator_2022

Fig. 3 Clustering results on three Elevator datasets with or without side information. The first three have no side information, the last three have side information.

the subspace representation matrices of different views into a tensor, where the low-rank constraint could capture the global structure of raw data.

- Compared with the nearest neighbor algorithm (MLAN, MVGL), MLAN simply fuses multiple similarity matrices. MVGL uses a weighted fusion of multiple similarity matrices. Our TMSCS uses $l_{2,1}$norm to remove the noise from each view and stacks multiple representation matrices into a tensor, using Tucker decomposition to uniformly explore the low-rank properties of the tensor. This yields cleaner representations to learn an affinity matrix. So

Table 3 CLUSTERING RESULTS (MEAN±STANDARD DEVIATION).

Dataset	Method	NMI	ACC	AR
ORL(K=10)	CLRR *(TCYB2016)*	0.917±0.008	0.862±0.013	0.764±0.027
	CNMF *(TPNMI2016)*	0.695±0.005	0.527±0.016	0.387±0.011
	MVGL *(TCYB2017)*	0.804±0.000	0.781±0.000	0.722±0.000
	MLAN *(AAAI2017)*	0.830±0.001	0.684±0.001	0.331±0.001
	TMSRL *(IJCV2020)*	0.964±0.006	0.909±0.015	0.879±0.018
	LRTG *(TCSVT2021)*	0.967±0.000	0.922±0.000	0.896±0.000
	TMSCS	**0.988±0.000**	**0.985±0.000**	**0.969±0.000**
BBCSport(K=20)	CLRR *(TCYB2016)*	0.787±0.000	0.921±0.000	0.816±0.000
	CNMF *(TPNMI2016)*	0.580±0.132	0.645±0.104	0.392±0.166
	MVGL *(TCYB2017)*	0.820±0.000	0.857±0.000	0.759±0.000
	MLAN *(AAAI2017)*	0.794±0.000	0.728±0.000	0.606±0.000
	TMSRL *(IJCV2020)*	0.846±0.000	0.947±0.000	0.864±0.000
	LRTG *(TCSVT2021)*	0.757±0.000	0.818±0.000	0.673±0.000
	TMSCS	**0.989±0.000**	**0.996±0.000**	**0.995±0.000**
MSRC_v1(K=20)	CLRR *(TCYB2016)*	0.896±0.000	0.952±0.000	0.891±0.000
	CNMF *(TPNMI2016)*	0.666±0.027	0.727±0.065	0.571±0.050
	MVGL *(TCYB2017)*	0.698±0.000	0.819±0.000	0.622±0.000
	MLAN *(AAAI2017)*	0.662±0.000	0.681±0.000	0.504±0.000
	TMSRL *(IJCV2020)*	0.921±0.000	0.962±0.000	0.914±0.000
	LRTG *(TCSVT2021)*	0.830±0.000	0.895±0.000	0.775±0.000
	TMSCS	**0.968±0.000**	**0.986±0.000**	**0.966±0.000**
Elevator_WX(K=25)	CLRR *(TCYB2016)*	0.830±0.000	0.980±0.000	**0.940±0.000**
	CNMF *(TPNMI2016)*	0.577±0.214	0.941±0.078	0.574±0.260
	MVGL *(TCYB2017)*	**0.836±0.000**	0.902±0.000	0.796±0.000
	MLAN *(AAAI2017)*	0.569±0.000	0.944±0.000	0.536±0.000
	TMSRL *(IJCV2020)*	0.801±0.000	0.965±0.000	0.848±0.000
	LRTG *(TCSVT2021)*	0.578±0.000	0.975±0.000	0.691±0.000
	TMSCS	0.669±0.000	**0.983±0.000**	0.753±0.000
Elevator_CX(K=20)	CLRR *(TCYB2016)*	0.780±0.000	0.958±0.000	0.822±0.000
	CNMF *(TPNMI2016)*	0.599±0.272	0.902±0.096	0.567±0.375
	MVGL *(TCYB2017)*	0.820±0.000	0.857±0.000	0.759±0.000
	MLAN *(AAAI2017)*	0.189±0.014	0.959±0.002	0.328±0.019
	TMSRL *(IJCV2020)*	0.518±0.000	0.964±0.000	0.683±0.000
	LRTG *(TCSVT2021)*	**0.759±0.000**	0.932±0.000	**0.845±0.000**
	TMSCS	0.352±0.000	**0.974±0.000**	0.405±0.000

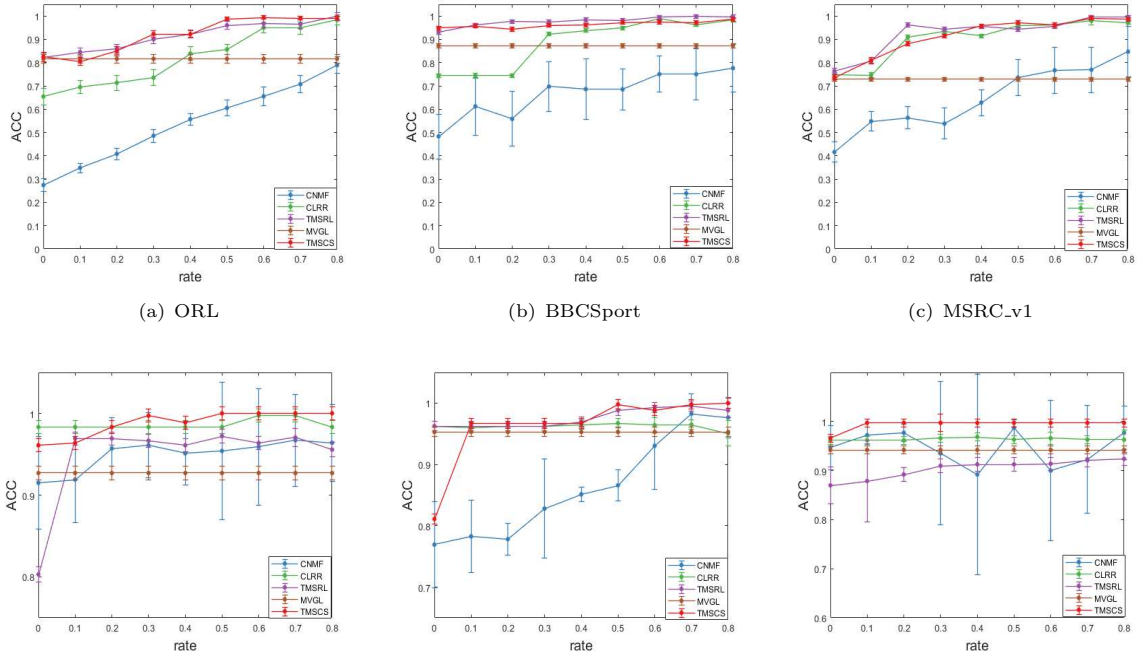

(a) ORL (b) BBCSport (c) MSRC_v1

(d) Elevator_WX (e) Elevator_CX (f) Elevator_2022

Fig. 4 Results of TMSCS and other algorithms with different label proportion.

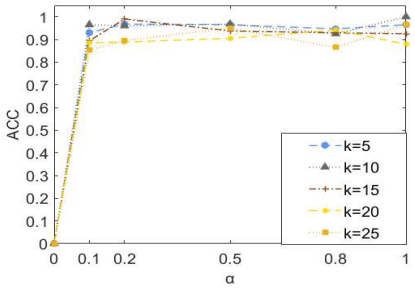

(a) Result on ORL dataset with different α

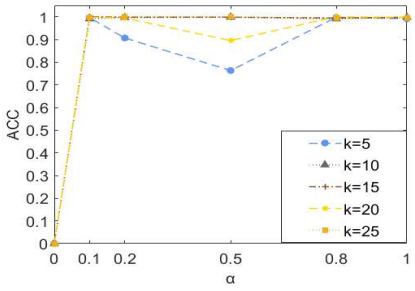

(b) Result on BCCSport dataset with different α

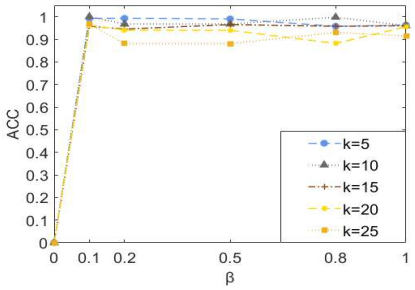

(c) Result on ORL dataset with different β

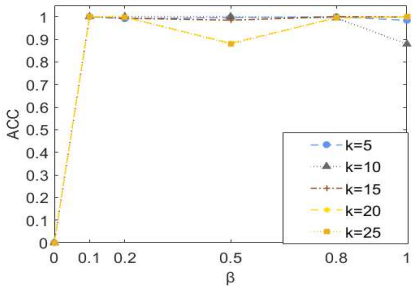

(d) Result on BCCSport dataset with different β

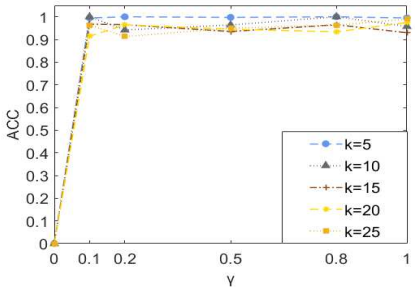

(e) Result on ORL dataset with different γ

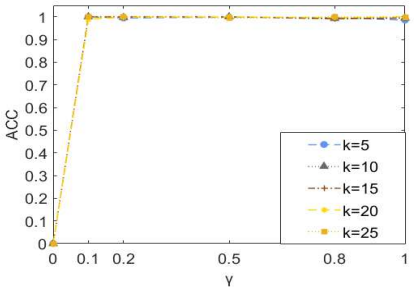

(f) Result on BCCSport dataset with different γ

Fig. 5 Performance of TMSCS with different values of α, β and γ.

the ACC effect of TMSCS is improved by 29% and 14%, respectively.

4.4 Results on elevator status datasets

We conducted further experiments on elevator datasets. The corresponding clustering results are shown in Fig.3: The blue, red and green points represent devices with different risk levels. Regions are divided according to device similarity. We randomly take several samples on the cluster boundaries, and if these samples all belong to low-risk devices in realistic scenarios, then we can determine that all samples within the same cluster are low-risk devices. If a new device is added to this cluster, it can be inferred that this device is low risk. In addition, a comparison with other semi-supervised algorithms (TMSRL, CNMF, CLRR) is performed, and the average ACC value is taken for 10 runs, and the line segment at the point in the graph represents the standard deviation. MVGL is used as the unsupervised base algorithm. The specific results are shown in Fig.4, and it can be seen that the corresponding ACC index has a significant improvement with the increase of side

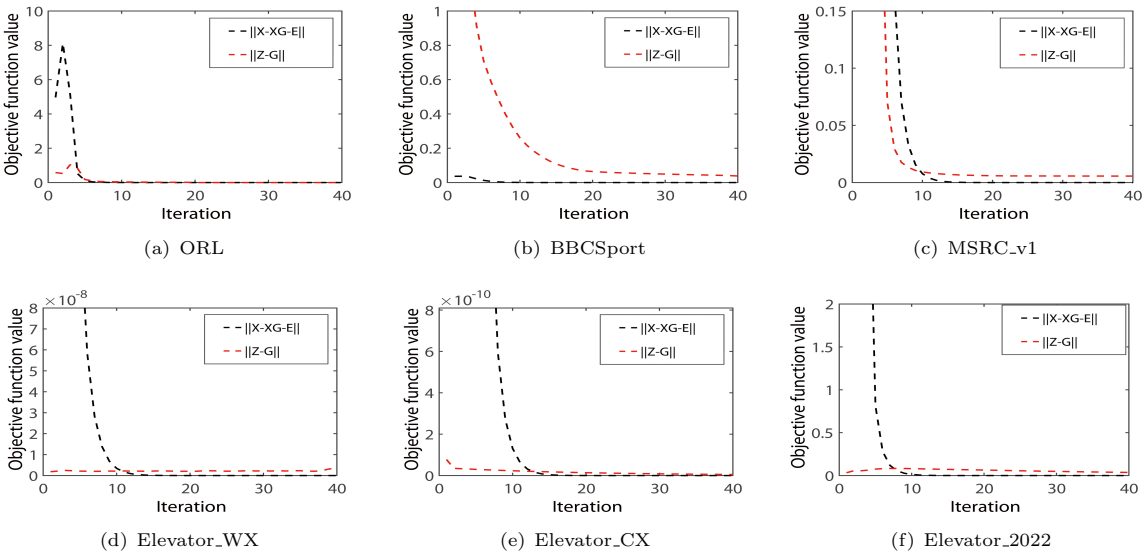

(a) ORL (b) BBCSport (c) MSRC_v1

(d) Elevator_WX (e) Elevator_CX (f) Elevator_2022

Fig. 6 Convergence curves over different datasets.

information. It indicates that the addition of side information can improve the clustering effect.

4.5 Parameter analysis

In this paper, there are six parameters in the algorithm: α, β, γ, k, $rank$, and $rate$. α is selected from the set [0.1, 0.2, 0.5, 0.8, 1] to control the noise matrix. β is selected from the set [0.1, 0.2, 0.5, 0.8, 1] to control the difference between the target similarity matrix and hybird matrix. γ is selected from the set [0.1, 0.2, 0.5, 0.8, 1] to control the Laplace matrix. k is used to control the number of neighbors. $rank$ is used to control the rank of tensor and set $rank = [50, 50, m]$. 50 is the dimension. m is the number of views. The $rate$ represents the percentage of side information. The $rate$ is set to 10% for TMSCS and 40% for the remaining semi-supervised algorithms. The Fig.5 shows the results of ACC with different values of α, β, γ and k on two public datasets.

4.6 Convergence analysis

To verify the convergence of TMSCS, Fig.6 shows the convergence of the algorithm in this paper on each dataset. In each plot, the x-axis and y-axis indicate the number of iterations and the corresponding objective function values, respectively. It can be observed that the curve reaches convergence in about 15 iterations and then becomes stable as the number of iterations increases. It proves that our algorithm can converge quickly and stably in practice.

5 Conclusion

In this paper, a novel Tensorial Multi-view Subspace Clustering with Side Constraints (TMSCS) is proposed for elevator security warning, which incorporates tensorial multi-view subspace learning and adaptive graph learning to construct a unified model. The low signal-to-noise ratio problem in multi-view elevator status data is overcome with the help of tensor low-rank constraint. Meanwhile, the prior knowledge is formalized as side constraints between samples through adaptive graph learning, which significantly improves the clustering performance. Experiments on several benchmark datasets verify the superiority of the proposed method. In addition, the experimental results on three real elevator status datasets show that the proposed method can effectively identify the abnormal elevator equipments.

Acknowledgments. This word was supported by the National Natural Science Foundation of China (62206094), Zhejiang Market Supervision Administration Scientific Research Project (ZC2021B076), Huzhou Public Welfare Applied Research Project (2021GZ05).

References

[1] Van, L., Lin, Y., Wu, T., Lin, Y.: An intelligent elevator development and management system. IEEE Syst. J. **14**(2), 3015–3026 (2020)

[2] Zhao, B., Quan, Z., Li, Y., Quan, L., Hao, Y., Ding, L.: A hybrid-driven elevator system with energy regeneration and safety enhancement. IEEE Trans. Ind. Electron. **67**(9), 7715–7726 (2020)

[3] Oya, J.R.G., Fort, E.H., Chavero, F.M., Carvajal, R.G.: Compressive-sensing-based reflectometer for sparse-fault detection in elevator belts. IEEE Trans. Instrum. Meas. **69**(4), 947–949 (2020)

[4] Jiang, X., Huang, X., Huang, J., Tong, Y.: Real-time intelligent elevator monitoring and diagnosis: Case studies and solutions with applications using artificial intelligence. Comput. Electr. Eng. **100**, 107965 (2022)

[5] Brbić, M., Kopriva, I.: Multi-view low-rank sparse subspace clustering. Pattern Recognition **73**, 247–258 (2018)

[6] Zhan, K., Zhang, C., Guan, J., Wang, J.: Graph learning for multiview clustering. IEEE Trans. Cybern. **48**(10), 2887–2895 (2018)

[7] Zhang, C., Fu, H., Liu, S., Liu, G., Cao, X.: Low-rank tensor constrained multiview subspace clustering. In: Proceedings of IEEE International Conference on Computer Vision, ICCV, pp. 1582–1590 (2015)

[8] Xie, Y., Tao, D., Zhang, W., Liu, Y., Zhang, L., Qu, Y.: On unifying multi-view self-representations for clustering by tensor multi-rank minimization. Int. J. Comput. Vis. **126**(11), 1157–1179 (2018)

[9] Chen, Y., Xiao, X., Peng, C., Lu, G., Zhou, Y.: Low-rank tensor graph learning for multiview subspace clustering. IEEE Trans. Circuits Syst. Video Technol. **32**(1), 92–104 (2022)

[10] Wang, S., Chen, Y., Jin, Y., Cen, Y., Li, Y., Zhang, L.: Error-robust low-rank tensor approximation for multi-view clustering. Knowl. Based Syst. **215**, 106745 (2021)

[11] Nie, F., Cai, G., Li, X.: Multi-view clustering and semi-supervised classification with adaptive neighbours. In: Proceedings of the 31th AAAI Conference on Artificial Intelligence, pp. 2408–2414 (2017)

[12] Zhang, C., Zheng, B., Tsung, F.: Multi-view metro station clustering based on passenger flows: a functional data-edged network community detection approach. Data Min. Knowl. Discov. **37**(3), 1154–1208 (2023)

[13] Wang, Q., Chen, M., Nie, F., Li, X.: Detecting coherent groups in crowd scenes by multiview clustering. IEEE Trans. Pattern Anal. Mach. Intell. **42**(1), 46–58 (2020)

[14] Wang, H., Sun, M.: Smart-vposenet: 3d human pose estimation models and methods based on multi-view discriminant network. Knowledge-Based Systems **239**, 107992 (2022)

[15] Yan, K., Lv, H., Guo, Y., Chen, Y., Wu, H., Liu, B.: Tppred-atmv: therapeutic peptide prediction by adaptive multi-view tensor learning model. Bioinformatics **38**(10), 2712–2718 (2022)

[16] Zhang, F., Yin, H., Cheng, X., Du, W., Xu, H.: LSMVC: low-rank semi-supervised multiview clustering for special equipment safety warning. In: Proceedings of the 28th International Conference on Neural Information Processing, ICONIP, vol. 13109, pp. 3–14 (2021)

[17] Xie, D., Gao, Q., Yang, M.: Enhanced tensor low-rank representation learning for multiview clustering. Neural Networks **161**, 93–104 (2023)

[18] Guo, J., Sun, Y., Gao, J., Hu, Y., Yin, B.: Logarithmic schatten-p p norm minimization for tensorial multi-view subspace clustering. IEEE Trans. Pattern Anal. Mach. Intell. **45**(3), 3396–3410 (2023)

[19] Chen, M., Wang, C., Lai, J.: Low-rank tensor based proximity learning for multi-view clustering. IEEE Trans. Knowl. Data Eng. **35**(5), 5076–5090 (2023)

[20] Tang, Y., Xie, Y., Zhang, C., Zhang, Z., Zhang, W.: One-step multiview subspace segmentation via joint skinny tensor learning and latent clustering. IEEE Trans. Cybern. **52**(9), 9179–9193 (2022)

[21] Bo, X., Kang, Z., Zhao, Z., Su, Y., Chen, W.: Latent multi-view semi-supervised classification. In: Proceedings of the 11th Asian Conference on Machine Learning, ACML, vol. 101, pp. 348–362 (2019)

[22] Zhou, H., Yin, H., Li, Y., Chai, Y.: Multiview clustering via exclusive non-negative subspace learning and constraint propagation. Inf. Sci. **552**, 102–117 (2021)

[23] Liang, N., Yang, Z., Li, Z., Xie, S., Sun, W.: Semi-supervised multi-view learning by using label propagation based non-negative matrix factorization. Knowl. Based Syst. **228**, 107244 (2021)

[24] Elhamifar, E., Vidal, R.: Sparse subspace clustering. In: Proceedings of IEEE Conference on Computer Vision and Pattern Recognition CVPR, pp. 2790–2797 (2009)

[25] Liu, G., Lin, Z., Yu, Y.: Robust subspace segmentation by low-rank representation. In: Proceedings of the 27th International Conference on Machine Learning ICML, pp. 663–670 (2010)

[26] Xu, H., Zhang, X., Xia, W., Gao, Q., Gao, X.: Low-rank tensor constrained co-regularized multi-view spectral clustering. Neural Networks **132**, 245–252 (2020)

[27] Wang, C., Geng, L., Zhang, J., Wu, T.: Multiview clustering via robust consistent graph learning. Digit. Signal Process. **128**, 103607 (2022)

[28] Zhang, C., Fu, H., Wang, J., Li, W., Cao, X., Hu, Q.: Tensorized multi-view subspace representation learning. Int. J. Comput. Vis. **128**(8), 2344–2361 (2020)

[29] Nie, F., Wang, X., Huang, H.: Clustering and projected clustering with adaptive neighbors. In: Proceedings of the 20th International Conference on Knowledge Discovery and Data Mining, KDD, pp. 977–986 (2014)

[30] Liu, G., Lin, Z., Yan, S., Sun, J., Yu, Y., Ma, Y.: Robust recovery of subspace structures by low-rank representation. IEEE Trans. Pattern Anal. Mach. Intell. **35**(1), 171–184 (2013)

[31] Sheehan, B.N., Saad, Y.: Higher order orthogonal iteration of tensors (HOOI) and its relation to PCA and GLRAM. In: Proceedings of the 7th SIAM International Conference on Data Mining, pp. 355–365 (2007)

[32] Wang, D., Nie, F., Huang, H.: Feature selection via global redundancy minimization. IEEE Trans. Knowl. Data Eng. **27**(10), 2743–2755 (2015)

[33] Liu, H., Wu, Z., Li, X., Cai, D., Huang, T.S.: Constrained nonnegative matrix factorization for image representation. IEEE Trans. Pattern Anal. Mach. Intell. **34**(7), 1299–1311 (2012)

[34] Wang, J., Wang, X., Tian, F., Liu, C.H., Yu, H.: Constrained low-rank representation for robust subspace clustering. IEEE Trans. Cybern. **47**(12), 4534–4546 (2017)